THE ELECTRON GUN FOR THE STANFORD TWO-MILE ACCELERATOR*

R. H. Miller, J. Berk, T. O. McKinney
Stanford Linear Accelerator Center, Stanford University, Stanford, California

Summary

The design of the electron gun for an electron linear accelerator is of prime importance in achieving a small emittance volume and good reliability. This paper discusses phase space concepts useful in gun design, the design of the SLAC electron gun, and tests of its performance. A convenient definition for the effective area in phase space of a finite set of calculated points is proposed and a discussion of the increase in transverse phase space within a linear accelerator is presented. The SLAC gun is a Pierce spherical triode with a 50-ohm coaxial input to the grid. The gun is designed to operate with 80 kV dc between the cathode and the anode. The current in the beam can be varied from 2 A peak to less than 10^{-8} A peak by varying the grid to cathode voltage over a range of about 1000 volts. The design permits use of either an oxide cathode radiantly heated or a thoriated tungsten cathode heated by electron bombardment.

Phase Space Concepts in Gun Design

The ease with which a high energy particle beam can be transported over long distances, the precision with which the beam energy can be measured, and the precision with which scattering angles of particles can be determined in a physics experiment all depend on the transverse phase space area (or emittance) of the beam. The emittance of an electron linear accelerator is largely determined by the emittance of the electron gun. Thus, the quality of the gun influences beam transport systems and the resolution of physics experiments carried out using the beam.

Two apertures of radius r_1 and r_2 separated a distance L define a beam radius r_1 and a radial momentum interval

$$p_r = \frac{r_2 p}{L} ,$$

where p is the momentum of the particles. The area of the inscribed ellipse is

$$A = \frac{\pi r_1 r_2 p}{L} , \qquad (1)$$

which is commonly defined as the admittance of two apertures. If the particles are accelerated from an energy of γ_1 at the first aperture to γ_2 at the second, the admittance is

$$A = \frac{\pi r_1 r_2 p}{\left[\left(\frac{\gamma_1}{\gamma_2 - \gamma_1}\right) \ell n \frac{\gamma_2}{\gamma_1}\right] L} . \qquad (2)$$

At SLAC, the accelerator beam transport system was designed with a focusing element about every 100 meters. The beam enters this system with an energy of .6 GeV and gains about .6 GeV in 100 meters. The radius of the accelerator aperture is 0.86 cm. The admittance of the accelerator is determined by this first standard 100-meter sector. To allow for missteering, misalignment, and stray fields, it was decided to limit the beam diameter to 1/2 the accelerator aperture. Therefore the maximum allowable beam emittance is $A_{beam} = 0.1$ in units of $m_o c$ cm.

Thermal velocities at the cathode, production imperfections in the gun, the lens effect of each individual aperture in the grid mesh, aberrations in the electrostatic focusing of the gun and the RF fields used to bunch and accelerate the beam all contribute to the emittance of the accelerator. No attempt will be made to evaluate the effect of imperfections and grid structure. The contribution of thermal velocities at the cathode is discussed first, some fairly crude estimates of the RF effects next, and the aberrations of the electrostatic focusing are discussed in the section on computer design of the gun.

Thermal Velocity Effects

The minimum emittance a gun can have is determined by the area and temperature of the cathode. The electrons emitted from the cathode have a mean square transverse velocity due to thermal energy given by

$$\overline{v_r^2} = \frac{kT}{m_o} ;$$

so the emittance area due to thermals is

$$A_T = \pi r_c \sqrt{\frac{kT}{m_o c^2}} \qquad (3)$$

where r_c is the cathode radius.

For thermal electron emitters kT varies from ≈ 0.1 eV for oxide to ≈ 0.2 eV for pure metal emitters and the cathode radius in the SLAC gun is approximately 1 cm so the minimum emittance achievable is

$$A_T \approx 1 \times 10^{-3} \; m_o c \text{ cm} .$$

RF Field Effects

The rate of change of radial momentum (units of $m_o c$) due to RF accelerating fields is given by the Lorenz force

$$\frac{dp_r}{dt} = \frac{e}{m_o c} \left(E_r - v_z B_\phi\right) . \qquad (4)$$

Replacing dt by $\frac{1}{\beta c} dz$, using the Maxwell equations the following normalized variables

$\rho = r/\lambda$ $\qquad$ $\beta_w = v_p/c$

$Z = z/\lambda$ $\qquad$ $\beta = v/c$ for the electron

$\alpha = \frac{eE\lambda}{m_o c^2}$ $\qquad$ $\gamma = \frac{1}{\sqrt{1-\beta^2}}$

one obtains the radial equation of motion[1]

$$\frac{dp_r}{dZ} = \pi \alpha \rho \left(\frac{1}{\beta_w \beta} - 1\right) \cos\theta + \frac{\rho}{2\beta} \frac{\partial \alpha}{\partial Z} \sin\theta , \qquad (5)$$

for $p \ll 1$.

*Work supported by the U.S. Atomic Energy Commission.

The first cos θ term is due to the radial electric fields in the interior of the structure, the second cos θ term is due to the azimuthal magnetic fields, and the third term represents fringing fields at the input and the output of the structure. The origin for the phase angle θ is the longitudinal field null forward of the accelerating crest (i.e. the phase stable null).

In the same units the longitudinal equations of motion[1,2] are

$$\frac{d\gamma}{dZ} = -\alpha \sin\theta \quad \text{(a)} \qquad \frac{d\theta}{dZ} = 2\pi\left(\frac{1}{\beta_w} - \frac{1}{\beta}\right) \quad \text{(b)} \tag{6}$$

The radial equation of motion, Eq. (5), can be easily evaluated using an impulse approximation for the case of injecting nonrelativistic electrons directly into an accelerator section with α constant, $\beta_w = 1$.

The cos θ vanishes on the crest and furthermore the factor $(1-\beta)/\beta$ diminishes as $1/2\gamma^2$, so the first term in Eq. (5) decreases very rapidly with increasing Z. The $\partial\alpha/\partial Z$ term is a significant contribution to emittance only at the input fringing field where there are electrons distributed over a wide range of sin θ values. Consequently, an impulse approximation in which the radius ρ is assumed to be constant during the time when the radial forces are applied is accurate enough to be useful. Substituting Eq. (6b) into Eq. (5) for the case $\beta_w = 1$ gives

$$dp_r = -\alpha \frac{\rho}{2} \cos\theta \, d\theta + \frac{\rho}{2} \sin\theta \, d\alpha \ .$$

If one sets $\rho = \rho_o$ this is integratable yielding for

$$\beta_w = 1: \ \Delta p_r = \frac{\alpha\rho_o}{2}\left[1 + \left(1 + \frac{1}{\beta_o}\right) \sin\theta_o\right] ; \tag{7}$$

where it is assumed that the electrons are on the crest at the end of the integration interval.

Equation (7) is very useful in understanding and estimating the radial optics of a non-relativistic electron entering a linear accelerator. The electrons experience a radially defocusing force which is strongly dependent on their entering phase θ_o. Figure 1 illustrates this RF lens effect computed by numerical integration of the equations of motion through the first two wavelengths of the SLAC accelerator in which $\alpha = 2.4$, $\beta_w = 1.0$, $\beta_o = 0.75$.

A comparison of the computer calculations with the impulse approximation (Eq. 7) shows reasonable agreement:

$$\text{Computer } \Delta p_r = (1.4 + 3.7 \sin\theta_o)\rho_o \ ,$$

$$\text{Impulse approximation } \Delta p_r = (1.2 + 2.8 \sin\theta_o)\rho_o \ .$$

Because the radial forces depend on phase, they produce an increase in the radial emittance. A similar analysis can be done for a short buncher in which

$$\beta_w < 1; \ \Delta p_r \approx \frac{\alpha\rho_o}{2} \frac{\beta_w\left(1-\beta_o^2\right)}{\beta_o(\beta_w - \beta_o)} \left(\sin\theta_o - \sin\theta_1\right) \tag{8}$$

where θ_1 is the phase of the electron leaving the structure.

Finally, for a prebuncher if one assumes it has pure TM_{010} mode fields, the result is

$$\text{Prebuncher: } \Delta p_r \approx \pi\rho_o \Delta\gamma \left(\frac{1-\beta_o^2}{\beta_o^2}\right) \cos\theta_m \tag{9}$$

where $\Delta\gamma$ is the peak cavity voltage in units $\frac{m_o c^2}{e}$, and θ_m is the phase of the electron at the middle of the cavity. In each of these structures there is an increase in the transverse phase area which is given by

$$\Delta A \approx \pi\rho_o\lambda \frac{d(\Delta p_r)}{d\theta_o} \Delta\theta_o \ . \tag{10}$$

But the minimum radius which can be maintained through a region of length L can be expressed in terms of the emittance A using Eq. (1):

$$\rho = \frac{r}{\lambda} = \frac{1}{\lambda}\sqrt{\frac{AL}{\pi p}} \tag{11}$$

Combining Eqs. (10) and (11) with Eqs. (7), (8), (9) respectively, one obtains the increase in emittance

$$\beta_w = 1: \ A_{out} = \left[1 + \frac{\alpha}{2}\left(\frac{1+\beta_o}{\beta_o^2}\right)\left(1-\beta_o^2\right)^{1/2} \frac{L}{\lambda}\Delta\theta_o\right] A_{in} \tag{12}$$

$$\beta_w < 1: A_{out} = \left[1 + \frac{\alpha}{2} \frac{\beta_w}{\beta_o^2(\beta_w - \beta_o)}\left(1-\beta_o^2\right)^{3/2} \frac{L}{\lambda}\Delta\theta_o\right] A_{in} \tag{13}$$

$$\text{Prebuncher: } A_{out} = \left[1 + \pi\Delta\gamma\left(\frac{1-\beta_o^2}{\beta_o^2}\right)^{3/2} \frac{L}{\lambda} \frac{\Delta\theta_m^2}{8}\right] A_{in} \tag{14}$$

For the SLAC injector which has a prebuncher, a one wavelength long buncher with $\alpha = .4$, $\beta_w = .75$ and an acceleration section with $\alpha = 2.4$, $\beta_w = 1$, the prebuncher increases the phase space by a negligible factor of 1.03, the buncher by 2.6 and the first accelerator section by 2.5 according to these formulas. The RF structures increase the emittance by a factor of 7 so the gun must have an emittance $\lesssim .01$ ($m_o c$ - cm).

Conceptual Design

The pulse characteristics of the accelerator beam are defined by the gun. The gun pulse could be produced by several systems the most common of which are the following: a diode with pulsed voltage and a temperature limited cathode; a diode with a temperature limited cathode and a beam deflection chopper; a space charge limited triode with a non-intercepting modulating anode; a space charge limited triode with an intercepting mesh grid.

Varying the gun cathode voltage to control the pulse amplitude is unsatisfactory because a changing gun beam energy is not compatible with tight bunching. The SLAC accelerator requires several decades of current change from pulse to pulse at rates up to 360 pps. This requirement rules out the control of current with a temperature limited cathode. The mesh grid was chosen over the nonintercepting modulating anode because it was believed that an order of magnitude higher gain could be achieved with a mesh grid. Anticipation of a need for rise and fall times in the order of a nanosecond favored a high gain triode.

The mesh grid was placed at the nominal one percent V_{AK} potential surface to achieve the highest gain

consistent with a mesh size to grid to cathode spacing ratio of about two and other practical considerations. The closer the mesh grid to the cathode the more significant to the beam optics are perturbations in the grid shape and spacing due to production and temperature effects.

Electrode Configuration

The gun electrode configuration was developed using a Poisson equation solving computer program written by W. B. Herrmannsfeldt.[3] The program calculates both halves of the gun design problem, namely the potential distribution and the electron trajectories by iterating between the two. The program begins by solving the Laplace equation in the gun (i.e. no charge density). It then calculates the cathode emission densities and electron trajectories for that Laplace potential distribution. Then the charge distribution resulting from the trajectory calculation is inserted in the potential solving subprogram and the process is iterated. With suitable damping (accomplished by averaging cathode emission between successive iterations) the calculation converges in about six iterations.

The gun was originally calculated as a spherical diode, and the electrode shapes were modified until the trajectories closely approximate that of an ideal spherical diode. The computed potentials along the beam edge agree with the analytic solution for a spherical diode to within 1% for over 90% of the distance from the cathode to the anode. The grid was added conforming closely to an equipotential surface in the vicinity of the beam. The computed electron trajectories in the triode are shown in Fig. 2. The computer program treats the grid as an equipotential with no interception of beam current.

The computer output includes the radius r and the slope dr/dz of each trajectory at the exit plane. This data is plotted in Fig. 3. In order to get a quantitative evaluation of various electrode configurations, it was necessary to calculate an effective emittance area for sets of discrete points like that shown in Fig. 3. The approach used was to calculate the center of the distribution on the r, dr/dz half plane. An area A_i associated with the i-th trajectory is defined to be the cross product between the center of the distribution $(\bar{r},\ \overline{dr/dz})$ and the i-th point $(r_i,\ dr_i/dz)$. This area, A_i, is illustrated in Fig. 3. The effective emittance area $A_\times$ is defined to be proportional to the root mean square value of the areas A_i weighted with the current densities J_i:

$$A_\times \equiv \frac{3\pi^2 p}{2}\left[\frac{\sum_i J_i\left\{\frac{dr_i}{dz}\left(\sum_j J_j r_j\right) - r_i\left(\sum_j J_j \frac{dr_j}{dz}\right)\right\}^2}{\sum_i J_i^3}\right]^{1/2}.$$

This definition for the emittance area of a number of discrete points has the following desirable characteristics:

1. It vanishes when the points lie on a straight line through the origin.
2. It approaches the area of the ellipse for a very large number of equally weighted points uniformly distributed in the interior of an ellipse.
3. It is invariant under linear transformations which conserve phase area such as that representing an aberrationless lens.

The computed electron trajectories have an effective emittance area of 3.5×10^{-3} m_oc cm. This is about 3 times the calculated emittance due to thermal velocities with an oxide cathode. Using the crude estimate of a seven-fold increase in emittance due to radial RF forces in the prebuncher, buncher and first accelerator section, one expects an injector emittance of 2.5×10^{-2} m_oc cm. The injector emittance was measured to be 2.5 to 3×10^{-2} m_oc cm over a wide range of currents.[4]

Gun Design and Performance

Figure 4 illustrates the physical configuration of the gun. On the right is the vacuum flange which is the mechanical and electrical interface with the grounded accelerator structure. On this flange is mounted the anode, removal of which permits access to the inner gun. On the left is the rear deck which operates at cathode potential and is separated from the vacuum flange by the alumina insulator. With the corona shields shown the gun can be operated at 100 kV dc without arcing. Potential plotting on a conductive paper analog permitted adjustment of the corona shield on the anode flange to limit the maximum potential gradient in the ceramic to less than 890 volts/mm.

The rear deck is a recessed vacuum wall penetrated by the two filament feedthroughs and the grid coaxial drive line. This 50-ohm line has its outer conductor at cathode potential and its inner conductor connected to the grid structure. Inside the vacuum envelope the rear deck provides a structural support for the inner gun.

The inner gun can be replaced as a unit requiring only that connections be replaced to the two filament leads and the grid. The mounting interface with the rear deck is the cathode deck on which the cathode assembly, the inner heat shields and the beam forming electrode are mounted. Two decks, each supported from the cathode deck with three insulated legs, support the grid structure and the bombarder.

The bombarder is a coaxial filament support structure made from molybdenum and alumina. Two tantalum screws for clamping the filament legs allow convenient but secure filament installations. With suitable spacers installed at the rear of the bombarder the distance of the filament from the back of the cathode can be adjusted permitting either bombardment or radiant heating of the cathode.

Grid

The 1% grid-cathode voltage placement chosen for the grid results in a grid-cathode spacing of 2.5 mm. The mesh is woven with .05 mm diameter molybdenum wires at 1 mm spacing resulting in an interception to total area ratio of 10%. The mesh disc is stress relieved at 1000° C brightness for one minute in a molybdenum jig, thereby forming it into a spherical surface. The individual wire ends are then spot welded to the supporting .18 mm thick molybdenum focus electrode in an assembly jig. When the cathode is oxide coated and is operated at a temperature of 950° C brightness, the grid temperature measures about 410° C.

Cathode

The design center beam requirements of 2 A at 80 kV result in a gun design perveance of $.0885 \times 10^{-6}$ $A/V^{3/2}$. A cathode diameter of 1.90 cm and area of 2.84 cm^2 requires a maximum homogenous emission density of .775 A/cm^2 (assuming 10% grid capture). This

emission level can, for a 2.5 μs pulse and a maximum .001 duty factor, be gotten from several emitter materials.[5]

The technology of thin film emitters applied to a conducting base as a mixture of barium, strontium, and, sometimes, calcium carbonates and later thermally converted to oxides is well developed and reliable. The first SLAC guns use this emitter material sprayed on a nickel cathode base. Bases with both a fine nickel mesh and a fine nickel powder diffusion bonded to the surface provide adequate bonding interfaces for the carbonates.

The cumbersome and sometimes slow conversion processes required and the sensitivity of these emitters to poisoning in vacuums worse than 10^{-5} mmHg has led SLAC to design the gun to accept a carburized tungsten cathode similar to that described by Haimson and Brodie.[6] The initial production of the .2 mm thick carburized layer using colloidal graphite is as involved as the oxide cathode but is done in the vacuum bell jar as this emitter can be exposed to air and reconverted (with a quick temperature flash) several times. It also requires a higher operating temperature. Whereas the oxide cathode operates at up to 900° C, the tungsten cathode requires up to 1600° C.

The effect of the higher temperature on the power required can be seen by calculating the power radiated by the electron emitting surface of the different cathodes. Assuming the cathodes face a cold wall with no additional heat shielding, the oxide cathode at 900° C radiates 10 watts while the tungsten cathode at 1600° C radiates 100 watts.

Filament

The oxide cathode temperatures can be easily achieved using a radiantly heating spiral filament. Heaters with .6 cm spacing between center leg and outer leg, 9-1/2 turns of .25 mm diameter tungsten 2% thoria wire and .50 mm turn-to-turn spacing have a resistance of about 2.57 ohms at 1720° C and, in the SLAC gun, require about 40 W to maintain the oxide cathode at 776° C brightness. The tungsten cathode requires about 150 W to 200 W to operate at 1600° C, depending on the bombarder emitter efficiency. This same filament is used but carburized and as a bombarder diode emitter.

The filaments are wound two at a time, interleaved and back-to-back, in a molybdenum jig. They are then stress relieved by heating to 1500° C brightness for two minutes in the vacuum bell jar. For use as electron emitters they are then carburized. They are sprayed with colloidal graphite in an aqueous solution and fired in vacuum to 1800° C brightness for 30 seconds.

In bombarder service these filaments are mounted one cm from the cathode back and with 1.4 kV applied between filament and cathode a bombarder beam current of 150 mA dc provides 210 W of beam power with only 5 W of applied filament power. The filament operates at a temperature of 1450° C with a cathode temperature of 1600° C but most of the power required to heat the filament is derived from the back heating from the hotter cathode. Control is maintained by controlling the applied filament power with a bombarder beam current signal and thereby the filament emitter is operated temperature limited.

Performance

The beam profiles shown in Fig. 5 were measured using a SLAC Model 4-1 gun with an oxide cathode and the SLAC beam analyzer. Cross sections of the beam current density were made using a .25 mm diameter hole in front of a small Faraday cup. The beam radii were then measured at 10% of the maximum current density. Thus the profiles should contain about 90% of the beam current.

The profiles illustrate a beam minimum diameter of .76 cm at about 2.5 cm downbeam from the gun vacuum flange for the 0.10 μperv ($\times 10^{-6}$ A/V$^{3/2}$) beam which is approximately the gun design perveance. Space charge spreading is an important effect at this perveance. The figure shows that the beam minimum moves back towards the cathode and becomes smaller with decreasing perveance.

The transfer characteristics shown in Fig. 6 were taken with a SLAC Model 4-2 gun with an oxide cathode at a cathode-anode voltage of 40 kV. Therefore, the 1% grid drive current of 1.2 A at 40 kV is a perveance of .15 μpervs. At 80 kV, this would give 3.4 A.

The cutoff level in Fig. 6 of 700 μA is determined by pulse noise in the system. Use of the gun on the SLAC accelerator has shown, however, that the cutoff current is below 10^{-8} A.

Acknowledgments

The authors wish to acknowledge the considerable contributions of the following: W. B. Herrmannsfeldt who wrote and ran the computer program; H. Hogg who did the initial mechanical design and participated in the choice of electrode configuration; W. Schultz who contributed his knowledge of materials and fabrication technique; J. Zinc who solved many problems in refractory metal fabrication and made most of the gun parts and jigs, and J. Crew who did the mechanical design and drafting.

References

1. E. L. Chu, "The Theory of Linear Accelerators," ML-140, Stanford University, Stanford, California, May 1951.

2. G. Dome, "Electron Bunching by Uniform Sections of Disc Loaded Waveguide," ML-242-A, Stanford University, Stanford, California, December 1960.

3. W. B. Herrmannsfeldt, "Poisson Equation Solving Program," SLAC Report 51, Stanford University, Stanford, California, September 1965.

4. R. H. Miller, "Measurement of the SLAC Injector Emittance," Proceedings of the 1966 Linear Accelerator Conference, October 3-7, 1966, LASL, Los Alamos, New Mexico (December 1963).

5. G. A. Haas, "Thermionic Electron Sources," Naval Research Labs Report 3657, October 6, 1961, Fig. 1, p. 5.

6. J. Haimson, I. Brodie, "High Current Cathode for Electron Linear Accelerator," Nature, 199, No. 4895, 795-797, August 24, 1966.

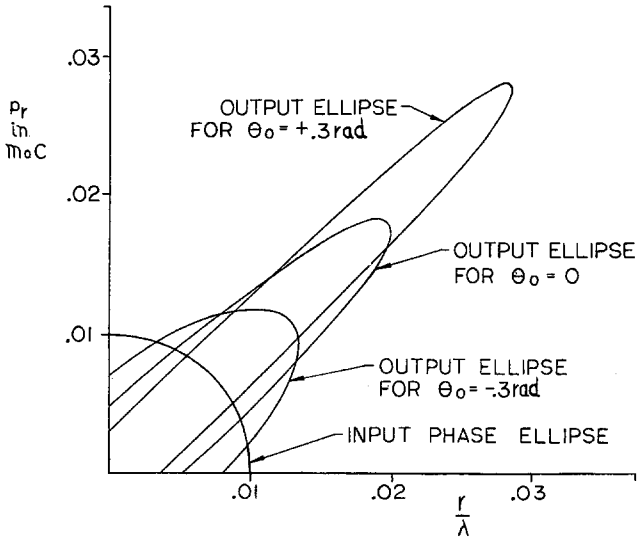

Fig. 1. Input and Output Phase Space for First 2 wavelengths of Accelerator, $\alpha = 2.4, \beta_w = 1, \beta_o = .75$.

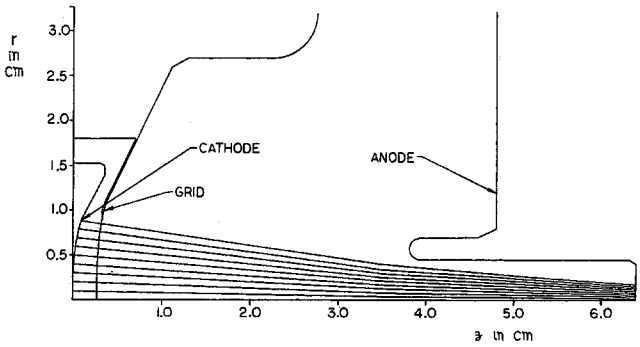

Fig. 2. Computer Electron Trajectories.

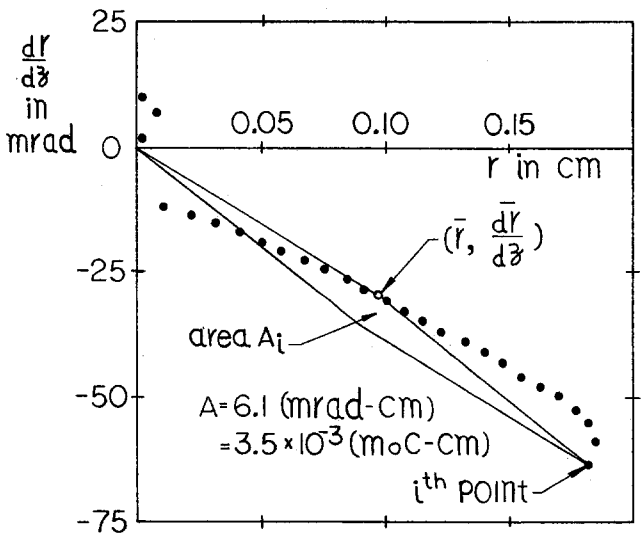

Fig. 3. Computed Gun Emittance.

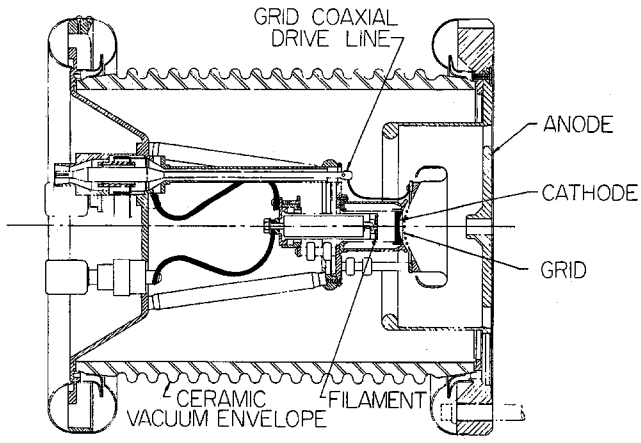

Fig. 4. Gun Assembly.

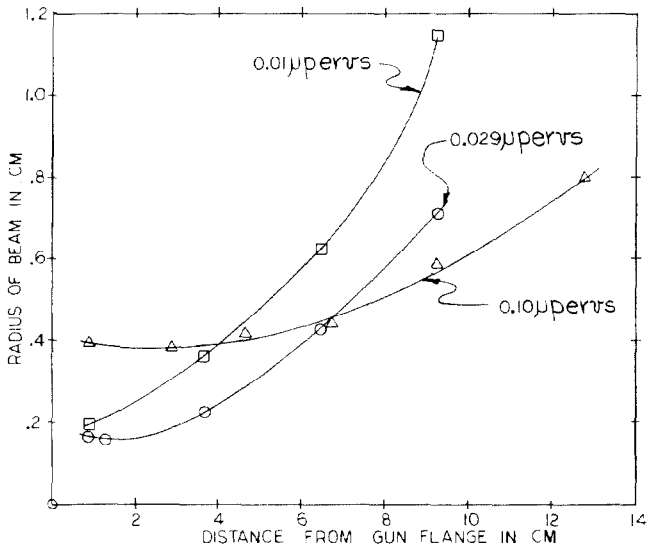

Fig. 5. Measured Beam Profiles.

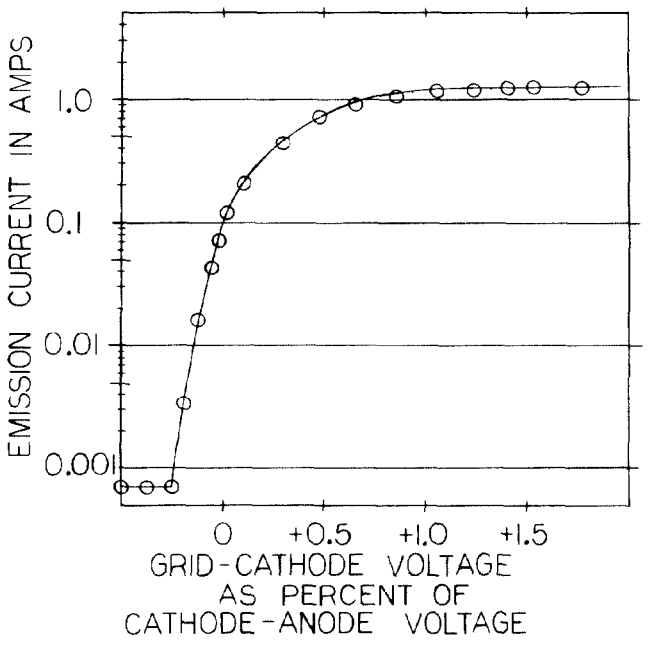

Fig. 6. Gun Transfer Characteristic.